

# All-optical switching in planar semiconductor microcavities

S. Schumacher,<sup>1</sup> N. H. Kwong,<sup>1</sup> R. Binder,<sup>1</sup> and Arthur L. Smirl<sup>2</sup>

<sup>1</sup>College of Optical Sciences, University of Arizona, Tucson, Arizona 85721, USA

<sup>2</sup>Laboratory for Photonics and Quantum Electronics,  
138 IATL, University of Iowa, Iowa City, Iowa 52242, USA

(Dated: November 1, 2018)

Using a microscopic many-particle theory, we propose all-optical switching in planar semiconductor microcavities where a weak beam switches a stronger signal. Based on four-wave-mixing instabilities, the general scheme is a semiconductor adaptation of a recently demonstrated switch in an atomic vapor [Dawes et al., Science 308, 672 (2005)].

PACS numbers: 190.4380, 320.7110, 190.3100

**INTRODUCTION** – In a recent study, an all-optical switch operating at very low light intensities was demonstrated in an atomic vapor system [1]. For two pump pulses counter-propagating through an atomic vapor, four-wave mixing (FWM) induced (spontaneous) off-pump-axis pattern formation can occur [2, 3, 4]. With a slight breaking of the system symmetry to impose a preferred direction to this off-axis pattern formation, it was demonstrated that a very weak “probe” pulse is sufficient to shift the patterns away from the preferred direction into the probe direction [1]. In this way, an all-optical switch was realized, where the switched signal is much stronger than the control pulse (in this case the probe).

A semiconductor version of that switch is desirable, and would be potentially useful in all-optical communication systems. In this Letter, we propose a specific implementation of such a switch. At the heart of our proposal is a planar semiconductor microcavity, in which FWM induced instabilities are already well established (see e.g., [5, 6, 7, 8, 9, 10]). The physical processes underlying instabilities in microcavities are quite different from instabilities found in atoms, and therefore, it is not trivial to transfer the atomic concepts to a semiconductor switch. In atoms, the dominant optical nonlinearity leading to FWM and instability is saturation (a process usually referred to as phase-space filling (PSF) in the semiconductor community). While in semiconductor microcavities, it is the repulsive Coulomb interaction between cavity polaritons. Despite the differences with atomic systems in terms of physics and geometry, we show that the microcavity still permits the same basic switching concept.

**THEORY** – We analyze the nonlinear cavity-polariton dynamics in a typical planar GaAs microcavity [11]. The linear polariton dispersion is shown in Fig. 1(a). Our theory is a  $\chi^{(3)}$  Hartree-Fock (HF) theory in the coherent limit, evaluated self-consistently up to arbitrary order in the optical fields [12, 13, 14, 15]. The polariton interactions are strongly spin-dependent [11, 16, 17, 18]. Here we concentrate on the dynamics in one spin subsystem (say spin up) by choosing circularly polarized excitation. We neglect a possible longitudinal-transverse (TE-TM) cavity-mode splitting [19]. We apply a spatial decompo-

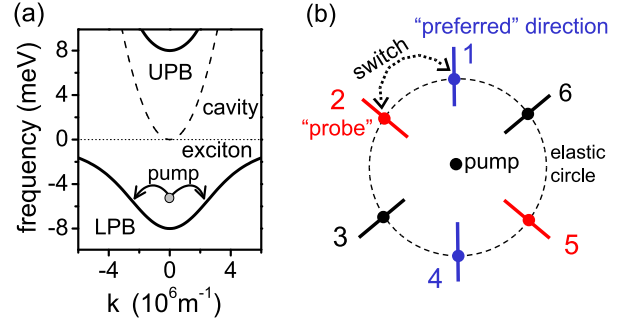


FIG. 1: (Color online) (a) Sketch of the linear cavity polariton dispersion. The bare cavity and exciton dispersions are shown, together with the lower (LPB) and upper (UPB) polariton branches of the coupled cavity-mode exciton system. The fundamental pairwise off-axis scattering of pump polaritons is also indicated. (b) Sketch of the hexagonal switching geometry in the transverse plane. The elastic circle is defined by the pump frequency and the dispersion of the LPB. The basic switching action triggered by the probe is indicated. The radial bars indicate the variation in the magnitude of off-axis momenta  $\mathbf{k}$  as included in the nonlinear polariton dynamics.

sition of cavity field and exciton polarization into Fourier components  $E_{\mathbf{k}}$  and  $p_{\mathbf{k}}$ , respectively, with in-plane momentum  $\mathbf{k}$  [20]. The exciton dynamics is evaluated in the 1s heavy-hole exciton subspace. The nonlinear set of coupled equations of motion for  $E_{\mathbf{k}}$  and  $p_{\mathbf{k}}$  reads [11, 20]:

$$i\hbar\dot{E}_{\mathbf{k}} = \hbar\omega_{\mathbf{k}}^c E_{\mathbf{k}} - \Omega_{\mathbf{k}} p_{\mathbf{k}} + i\hbar t_c E_{\mathbf{k},\text{inc}}^{\text{eff}}, \quad (1)$$

$$i\hbar\dot{p}_{\mathbf{k}} = (\varepsilon_{\mathbf{k}}^x - i\gamma_x) p_{\mathbf{k}} - \Omega_{\mathbf{k}} E_{\mathbf{k}} + \sum_{\mathbf{q}, \mathbf{k}''} (2\tilde{A}\Omega_{\mathbf{k}''} p_{\mathbf{q}}^* p_{\mathbf{k}'} E_{\mathbf{k}''} + V_{\text{HF}} p_{\mathbf{q}}^* p_{\mathbf{k}'} p_{\mathbf{k}''}) \delta_{\mathbf{q}, \mathbf{k}'+\mathbf{k}''-\mathbf{k}}. \quad (2)$$

The cavity-field in Eq. (1) is treated in quasi-mode approximation. The effective incoming field  $E_{\mathbf{k},\text{inc}}^{\text{eff}}$  driving the field  $E_{\mathbf{k}}$  in the cavity mode is obtained from a simple transfer-matrix formalism that includes the radiative width ( $\Gamma = \frac{\omega \hbar^2 t_c^2}{\varepsilon_0 c n_b}$ , with the background refractive index  $n_b$ , the vacuum velocity of light  $c$  and dielectric constant  $\varepsilon_0$ ) of the cavity mode and yields transmitted and re-

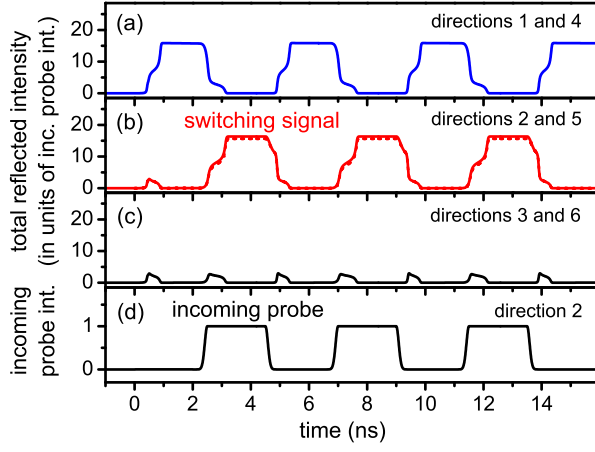


FIG. 2: (Color online) (a)-(c) Switching in the reflected signals. The intensities per direction are normalized to the incoming probe intensity. The switching signal in (b) is about 15 times stronger than the incoming probe in (d) that is triggering this signal (note the different scales on the vertical axes in panels (a)-(c) and (d)). In panel (b), direction 2 is shown as the solid line and direction 5 as the dashed line. Similar switching is observed in transmission (not shown).

flected field components:  $E_{\mathbf{k},\text{inc}}^{\text{eff}} = E_{\mathbf{k},\text{trans}} - E_{\mathbf{k},\text{refl}}$  with  $E_{\mathbf{k},\text{trans}} = E_{\mathbf{k},\text{inc}} + \frac{\hbar t_c}{2n_b c \epsilon_0} \dot{E}_{\mathbf{k}}$  and  $E_{\mathbf{k},\text{refl}} = -\frac{\hbar t_c}{2n_b c \epsilon_0} \dot{E}_{\mathbf{k}}$ . The cavity-to-outside coupling constant  $t_c$  is chosen such that  $\Gamma \approx 0.4$  meV for  $\hbar\omega = 1.5$  meV. We include excitonic PSF and HF exciton-exciton Coulomb interaction in the nonlinear exciton dynamics in Eq. (2); two-exciton correlations are neglected in this study and are expected to give merely quantitative changes because the pump is tuned far (several meV) below the bare exciton resonance [20, 21] (cf. Fig. 1(a)). Inclusion of two-exciton Coulomb correlations in our calculations would basically lead to renormalization of  $V_{\text{HF}}$  in Eq. (2) and give rise to a small additional excitation-induced dephasing [20, 21]. The bare exciton and cavity in-plane dispersions are denoted by  $\varepsilon_{\mathbf{k}}^x$  (with  $\varepsilon_0^x = 1.497$  eV) and  $\omega_{\mathbf{k}}^c$ , with  $\hbar\omega_{\mathbf{k}}^c = \varepsilon_0^x / \cos\vartheta$  and  $\sin\vartheta = |\mathbf{k}|c/(\omega n_b)$ . A phenomenological dephasing constant  $\gamma_x = 0.4$  meV is included for the exciton polarization,  $\Omega_{\mathbf{k}} = 8$  meV is the vacuum Rabi splitting, and  $\tilde{A} = A_{\text{PSF}}/\phi_{1s}^*(0)$  (with  $A_{\text{PSF}} = 4a_0^x\sqrt{2\pi}/7$ , the two-dimensional exciton Bohr radius  $a_0^x \approx 170 \text{ \AA}$ , and the two-dimensional 1s exciton wavefunction  $\phi_{1s}(\mathbf{r})$  at  $\mathbf{r} = 0$ ) and  $V_{\text{HF}} = 2\pi(1 - 315\pi^2/4096)/a_0^{x2}E_b^x$  (with the bulk exciton binding energy  $E_b^x \approx 13$  meV) are the excitonic PSF and HF Coulomb matrix elements, respectively. A spatial anisotropy in the system can be modeled, e.g., by including an anisotropic cavity dispersion  $\omega_{\mathbf{k}}^c$ .

We consider steady-state pump excitation in normal incidence ( $\mathbf{k}_{\text{pump}} = 0$ ), spectrally below the bare exciton resonance and above the lower polariton branch (cf. Fig. 1(a)). For this excitation configuration, FWM processes triggered by fluctuations in the cavity photon field

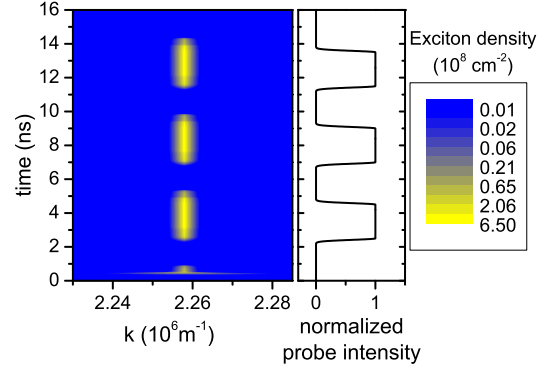


FIG. 3: (Color online) Timetrace of the exciton density in direction 2 in which the probe pulse is applied.

can give rise to resonant and phase-matched (momentum and energy conserving) pairwise off-axis scattering of pump-excited polaritons into two polaritons with finite and opposite in-plane momentum  $\mathbf{k}$  and  $-\mathbf{k}$  (cf. Fig. 1(a)). For a pump-induced exciton density above the instability threshold ( $\gtrsim 10^{10} \text{ cm}^{-2}$  here) these scattering processes can lead to strong off-axis signals as has been demonstrated in Ref. 10 for a slightly different excitation geometry. With a small symmetry breaking (anisotropy) in the system, hexagons and their subsets were shown to be the favored instability-induced patterns in [1].

In Eqs. (1) and (2), we allow for signals in the pump direction ( $\mathbf{k}_{\text{pump}} = 0$ ) and six off-axis directions forming hexagons in the transverse plane (cf. Fig. 1(b)). Contributions to  $E_{\mathbf{k}}$  and  $p_{\mathbf{k}}$  with finite in-plane momentum  $\mathbf{k} \neq 0$  (off-axis contributions) are restricted to  $k_{\text{min}} < |\mathbf{k}| < k_{\text{max}}$ . The lower ( $k_{\text{min}} \approx 2.0 \times 10^6 \text{ m}^{-1}$ ) and upper ( $k_{\text{max}} \approx 2.7 \times 10^6 \text{ m}^{-1}$ ) momentum cut-offs are chosen such that the elastic circle (including the dynamically changing nonlinear renormalizations) lies within the numerical domain. This approximation can be justified as long as the pump excitation takes place spectrally below the “magic angle” (analog to the experiments in [10]). Otherwise, energy and momentum conserving resonant scattering could significantly populate off-axis states away from the elastic circle.

**RESULTS & DISCUSSION** – In Figs. 2 and 3, we show results where we have numerically integrated the coupled Eqs. (1) and (2) for quasi steady-state pump excitation in normal incidence. The pump frequency is tuned 5 meV below the bare exciton resonance. The pump (not shown) reaches its peak intensity  $I_{\text{pump}} \approx 19.5 \text{ kWcm}^{-2}$  shortly after 0 ps and is then kept constant. We impose a slight anisotropy in the cavity dispersion by shifting  $\omega_{\mathbf{k}}^c$  to lower energies by 0.075 meV in directions 1 and 4. Above a certain pump threshold intensity, phase-matched pairwise scattering of pump-induced polaritons, driven mainly by the HF term in Eq. (2), leads to spontaneous (fluctuation-triggered) off-axis signal formation (similar to [10, 22]).

Initially, signals in all the considered off-axis directions start to grow simultaneously. However, as these signals grow over time, the anisotropy (symmetry breaking) fixes the spontaneous off-axis pattern at directions 1 and 4. This can be seen in Fig. 2(a)-(c) for times less than 2 ns. After 2 ns, we apply a weak probe ( $I_{\text{probe}} \approx 0.1 \text{ Wcm}^{-2}$ ) with the same frequency as the pump frequency in direction 2 (Fig. 2(d)). Now, the strong off-axis emission switches to directions 2 and 5 and vanishes in the “preferred” directions 1 and 4. Note that the switching signal in directions 2 and 5 is about *15 times stronger* than the probe pulse itself (i.e., part of the pump is redirected from normal incidence to the directions 2 and 5). In other words, the gain in direction 2 is  $\approx 11.7 \text{ dB}$ . When switching off the weak probe at  $\approx 5 \text{ ns}$ , the strong off-axis emission switches back to the preferred directions 1 and 4. The switching can then be repeated as shown in the figure. Finally, Fig. 3 shows the time evolution of the exciton density in direction 2 during the switching process. The density is resolved into its in-plane momentum components. For the chosen parameters the total off-axis density reaches about 10% of the pump-induced exciton density.

Figures 2 and 3 demonstrate the switching for one specific set of parameters. However, the general mechanism is robust. By fine-tuning the parameters in the relatively large parameter space that determines the system dynamics (e.g., pump and probe intensities and frequencies, and probe in-plane momentum), the switching performance shown in Figs. 2 and 3 can be optimized further, e.g., to achieve larger gain. Since the total strength of the off-axis signals is mainly determined by the pump excitation parameters, the largest gain is typically achieved for the lowest probe intensity that can trigger the switching process. We also note that the system dynamics drastically changes when the pump intensity and/or frequency is chosen such that bistability [23, 24] plays a role.

Finally, we briefly discuss possible limitations of the proposed scheme. Since the pump excitation is off-resonant, a relatively strong pump is required to reach the instability threshold. In an experimental setup, unintended off-axis scattering of pump light could reduce the contrast ratio between “on” and “off” states and thus the performance of the switch. However, this practical issue might be alleviated using another existing microcavity design [9] with a lower pump threshold intensity. We further note that in a fully two-dimensional simulation details of the switching process (e.g., the characteristic switching time) might change compared to the results in Fig. 2. Therefore, simulations beyond the hexagonal geometry considered in this work are desirable for the future.

**CONCLUSIONS** – We propose all-optical switching in planar semiconductor microcavities. Being based on four-wave mixing instabilities, the proposed scheme is similar to that recently demonstrated in an atomic vapor

[1]. Using a microscopic many-particle theory, our numerical simulations show that in the studied microcavity system a strong optical beam can be controlled with a weaker one. Besides its experimental verification, for the future it is worthwhile to study the influence of vectorial polarization effects [25] on the switching process, and to extend the analysis to other systems [9, 26].

**ACKNOWLEDGMENTS** – This work has been supported by ONR, DARPA, JSOP. S. Schumacher gratefully acknowledges support by the Deutsche Forschungsgemeinschaft through project No. SCHU 1980/3-1. Part of the computation was done at CCIT, University of Arizona.

- 
- [1] A. M. C. Dawes, L. Illing, S. M. Clark, and D. J. Gauthier, “All-optical switching in Rubidium Vapor,” *Science* **308**, 672 (2005).
  - [2] A. Yariv and D. M. Pepper, “Amplified reflection, phase conjugation, and oscillation in degenerate four-wave-mixing,” *Opt. Lett.* **1**(1), 16 (1977).
  - [3] G. Grynberg, “Mirrorless four-wave-mixing oscillation in atomic vapors,” *Optics Comm.* **66**(5,6), 321 (1988).
  - [4] R. Chang, W. J. Firth, R. Indik, J. V. Moloney, and E. M. Wright, “Three-dimensional simulations of degenerate counterpropagating beam instabilities in a nonlinear medium,” *Optics Comm.* **88**, 167 (1992).
  - [5] P. G. Savvidis, J. J. Baumberg, R. M. Stevenson, M. S. Skolnick, D. M. Whittaker, and J. S. Roberts, “Angle-resonant stimulated polariton amplifier,” *Phys. Rev. Lett.* **84**(7), 1547 (2000).
  - [6] C. Ciuti, P. Schwendimann, B. Deveaud, and A. Quattropani, “Theory of the angle-resonant polariton amplifier,” *Phys. Rev. B* **62**(8), R4825 (2000).
  - [7] M. Saba, C. Ciuti, J. Bloch, V. Thierry-Mieg, R. Andre, Le Si Dang, S. Kundermann, A. Mura, G. Bongiovanni, J. L. Staehli, and B. Deveaud, “High-temperature ultrafast polariton parametric amplification in semiconductor microcavities,” *Nature* **414**, 731 (2001).
  - [8] D. M. Whittaker, “Classical treatment of parametric processes in a strong-coupling planar microcavity,” *Phys. Rev. B* **63**, 193,305 (2001).
  - [9] C. Diederichs, J. Tignon, G. Dasbach, C. Ciuti, A. Lemaitre, J. Bloch, P. Roussignol, and D. Delalande, “Parametric oscillation in vertical triple microcavities,” *Nature* **440**, 904 (2006).
  - [10] M. Romanelli, C. Leyder, J. Ph. Karr, E. Giacobino, and A. Bramati, “Four wave mixing oscillations in a semiconductor microcavity: Generation of two correlated polariton populations,” *Phys. Rev. Lett.* **98**, 106,401 (2007).
  - [11] S. Schumacher, N. H. Kwong, and R. Binder, “Influence of exciton-exciton correlations on the polarization characteristics of the polariton amplification in semiconductor microcavities,” *Phys. Rev. B*, in press, arXiv.org:condmat/0708.1194v1 **76** (2007).
  - [12] M. Buck, L. Wischmeier, S. Schumacher, G. Czycholl, F. Jahnke, T. Voss, I. Rückmann, and J. Gutowski, “Light-polarization and intensity dependence of higher-order nonlinearities in excitonic FWM signals,” *Eur. Phys. J. B* **42**, 175 (2004).
  - [13] S. Schumacher, G. Czycholl, F. Jahnke, I. Kudyk, L. Wis-

- chmeier, I. Rückmann, T. Voss, J. Gutowski, A. Gust, and D. Hommel, “Coherent Propagation of Polaritons in Semiconductor Heterostructures: Nonlinear Pulse Transmission in Theory and Experiment,” *Phys. Rev. B* **72**(8), 081,308(R) (2005).
- [14] T. Östreich and L. J. Sham, “Collective Oscillations Driven by Correlation in the Nonlinear Optical Regime,” *Phys. Rev. Lett.* **83**(17), 3510 (1999).
- [15] S. Schumacher, N. H. Kwong, and R. Binder, “Large optical gain from four-wave mixing instabilities in semiconductor quantum wells,” *Europhys. Lett.* **81**, 27,003 (2008).
- [16] A. Kavokin, P. G. Lagoudakis, G. Malpuech, and J. J. Baumberg, “Polarization rotation in parametric scattering of polaritons in semiconductor microcavities,” *Phys. Rev. B* **67**, 195,321 (2003).
- [17] D. N. Krizhanovskii, D. Sanvitto, I. A. Shelykh, M. M. Glazov, G. Malpuech, D. D. Solnyshkov, A. Kavokin, S. Ceccarelli, M. S. Skolnick, and J. S. Roberts, “Rotation of the plane of polarization of light in a semiconductor microcavity,” *Phys. Rev. B* **73**, 073,303 (2006).
- [18] M. D. Martin, G. Aichmayr, A. Amo, D. Ballarini, L. Klotkowski, and L. Vina, “Polariton and spin dynamics in semiconductor microcavities under non-resonant excitation,” *J. Phys.: Condens. Matter* **19**, 295,204 (2007).
- [19] V. Savona, F. Tassone, C. Piermarocchi, A. Quattropani, and P. Schwendimann, “Theory of polariton photoluminescence in arbitrary semiconductor microcavity structures,” *Phys. Rev. B* **53**(19), 13,051 (1996).
- [20] S. Savasta, O. Di Stefano, and R. Girlanda, “Many-body and correlation effects on parametric polariton amplification in semiconductor microcavities,” *Phys. Rev. Lett.* **90**, 096,403 (2003).
- [21] N. H. Kwong, R. Takayama, I. Rumyantsev, M. Kuwata-Gonokami, and R. Binder, “Evidence of Nonperturbative Continuum Correlations in Two-Dimensional Exciton Systems in Semiconductor Microcavities,” *Phys. Rev. Lett.* **87**, 027,402 (2001).
- [22] A. Verger, I. Carusotto, and C. Ciuti, “Quantum Monte Carlo study of ring-shaped polariton parametric luminescence in a semiconductor microcavity,” *Phys. Rev. B* **76**, 115,324 (2007).
- [23] N. A. Gippius, S. G. Tikhodeev, V. D. Kulakovskii, D. N. Krizhanovskii, and A. I. Tartakovskii, “Nonlinear dynamics of polariton scattering in semiconductor microcavity: Bistability vs. stimulated scattering,” *Europhys. Lett.* **67**(6), 997 (2004).
- [24] M. Wouters and I. Carusotto, “Parametric oscillation threshold of semiconductor microcavities in the strong coupling regime,” *Phys. Rev. B* **75**, 075,332 (2007).
- [25] S. Schumacher, “Polarization-anisotropy induced spatial anisotropy of polariton amplification in planar semiconductor microcavities,” submitted, [arXiv.org:cond-mat/0711.0768v1](https://arxiv.org/abs/0711.0768v1) (2007).
- [26] S. Schumacher, N. H. Kwong, and R. Binder, “Polariton amplification in a multiple-quantum-well resonant photonic crystal,” submitted, [arXiv.org:cond-mat/0708.1300v1](https://arxiv.org/abs/0708.1300v1) (2007).